Dynamical and Thermal Problems in Vortex Development and Movement. Part II: Generalized Slantwise Vorticity Development

WU Guoxiong[1*] (吴国雄), ZHENG Yongjun[1,2] (郑永骏), and LIU Yimin[1] (刘屹岷)

1 *State Key Laboratory of Numerical Modeling for Atmospheric Sciences and Geophysical Fluid Dynamics, Institute of Atmospheric Physics, Chinese Academy of Sciences, Beijing* 100029

2 *Graduate University of the Chinese Academy of Sciences, Beijing* 100049

(Received March 28, 2012; in final form June 18, 2012)

ABSTRACT

The development of vertical vorticity under adiabatic condition is investigated by virtue of the view of potential vorticity and potential temperature (PV–θ) and from a Lagrangian perspective. A new concept of generalized slantwise vorticity development (GSVD) is introduced for adiabatic condition. The GSVD is a coordinate independent framework of vorticity development (VD), which includes slantwise vorticity development (SVD) when a particle is sliding down the concave slope or up the convex slope of a sharply tilting isentropic surface under stable or unstable condition. The SVD is a special VD for studying the severe weather systems with rapid development of vertical vorticity. In addition, the GSVD clarifies VD and SVD. The criteria for VD and SVD demonstrate that the demand for SVD is much more restricted than the demand for VD. When an air parcel is moving down the concave slope or up the convex slope of a sharply tilting isentropic surface in a stable stratified atmosphere with its stability decreasing, or in an unstable atmosphere with its stability increasing, i.e., its stability θ_z approaches zero, its vertical vorticity can develop rapidly if its C_D is decreasing.

The theoretical results are employed to analyze a Tibetan Plateau (TP) vortex (TPV), which appeared over the TP, then slid down and moved eastward in late July 2008, resulting in heavy rainfall in Sichuan Province and along the middle and lower reaches of the Yangtze River. The change of PV_2 contributed to the intensification of the TPV from 0000 to 0600 UTC 22 July 2008 when it slid upward on the upslope of the northeastern edge of the Sichuan basin, since the changes in both horizontal vorticity $\boldsymbol{\eta}_s$ and baroclinity $\boldsymbol{\theta}_s$ have positive effects on the development of vertical vorticity. At 0600 UTC 22 July 2008, the criterion for SVD at 300 K isentropic surface is satisfied, meaning that SVD occurred and contributed significantly to the development of vertical vorticity. The appearance of the stronger signals concerning the VD and SVD surrounding the vortex indicates that the GSVD concept can serve as a useful tool for diagnosing the development of weather systems.

Key words: potential vorticity, vorticity development, slantwise vorticity development, generalized slantwise vorticity development

Citation: Wu Guoxiong, Zheng Yongjun, and Liu Yimin, 2013: Dynamical and thermal problems in vortex development and movement. Part II: Generalized slantwise vorticity development. *Acta Meteor. Sinica*, **27**(1), 15–25, doi: 10.1007/s13351-013-0102-2.

1. Introduction

In Part I of this study (Zheng et al., 2013), the impacts of diabatic heating on the development and movement of vortex was investigated from a PV–Q and Lagrangian perspective, which showed that the inhomogeneity in both vertical and horizontal directions of condensation heating plays a leading role in the vortex's development and movement. As a follow-up, this study focuses on the vorticity development of a vortex under adiabatic constrain by revisiting the slantwise vorticity development (SVD) (Wu and Liu, 1997) from a PV–θ perspective. As presented in Part I, the vertical absolute vorticity per unit mass can be

Supported by the National Basic Research and Development (973) Program of China (2012CB417203 and 2010CB950403) and National Natural Science Foundation of China (40875034 and 40925015).

*Corresponding author: gxwu@lasg.iap.ac.cn.

Chinese version to be published.

©The Chinese Meteorological Society and Springer-Verlag Berlin Heidelberg 2013

expressed as

$$\eta_z = \frac{\mathrm{PV_e} - \mathrm{PV_2}}{\theta_z} = \frac{\mathrm{PV_e}}{\theta_z} - C_D,\ \theta_z \neq 0, \tag{1}$$

where

$$C_D = \frac{\mathrm{PV_2}}{\theta_z} = \frac{\boldsymbol{\eta}_s \cdot \boldsymbol{\theta}_s}{\theta_z},\ \theta_z \neq 0. \tag{2}$$

All notations used here and in the following are adopted from Part I (Zheng et al., 2013).

Based on the conservation of Ertel potential vorticity, Wu and Liu (1997) proposed the SVD theory to interpret the intense vertical vorticity development of a Lagrangian particle sliding down a slantwise isentropic surface. The condition for the SVD is also given in Wu and Liu (1997) and is duplicated here:

$$C_D(t+\Delta t) - C_D(t) < \mathrm{PV_e}\Big[\frac{1}{\theta_z(t+\Delta t)} - \frac{1}{\theta_z(t)}\Big]. \tag{3}$$

The SVD for a statically stable atmosphere was schematically explained by Wu and Liu (1997) for the downsliding case and by Cui et al. (2003) for an upsliding case.

Many applications of the SVD theory to diagnosing occurrences of torrential rain and severe weather obtained reasonable results and demonstrated that vertical vorticity can develop dramatically along the sharply sloping isentropic surface, and the condition $C_D < 0$ was diagnosed in some cases (Cui et al., 2002; Ma et al., 2002; Chen et al., 2004; Jiang et al., 2004; Wang et al., 2007). However, as shown in Eq. (1), the vertical vorticity development depends not only on C_D, but also on static stability θ_z under the conservation of $\mathrm{PV_e}$. From the definition of C_D in Eq. (2), a negative C_D under stable stratification implies a negative $\mathrm{PV_2}$. It was proved (Hoskins et al., 1985) that in the pressure coordinates $\mathrm{PV_2^p}$ is negative for geostrophic balance. In the height coordinates, the hydrostatic balance yields

$$\begin{cases} \dfrac{1}{\rho}\nabla_s p = \theta \nabla_s \pi, \\ \dfrac{\partial \pi}{\partial z} = -\dfrac{g}{\theta}, \end{cases} \tag{4}$$

where $\pi = C_p\Big(\dfrac{p}{p_0}\Big)^{R/C_p}$ is the Exner function. Then, the geostrophic wind in the height coordinates is

$$\boldsymbol{V}_\mathrm{g} = \frac{\boldsymbol{k}}{\rho f} \times \nabla_s p = \theta \frac{\boldsymbol{k}}{f} \times \nabla_s \pi. \tag{5}$$

Taking $\dfrac{\partial}{\partial z}$ on Eq. (5) yields the thermal wind

$$\begin{aligned} \frac{\partial \boldsymbol{V}_\mathrm{g}}{\partial z} &= \frac{\partial \theta}{\partial z}\frac{\boldsymbol{k}}{f} \times \nabla_s \pi + \theta \frac{\boldsymbol{k}}{f} \times \nabla_s \frac{\partial \pi}{\partial z} \\ &= \frac{\partial \theta}{\partial z}\frac{\boldsymbol{k}}{f} \times \nabla_s \pi + \frac{g}{\theta}\frac{\boldsymbol{k}}{f} \times \nabla_s \theta. \end{aligned} \tag{6}$$

Therefore,

$$\begin{aligned} \mathrm{PV_2} &= \alpha\Big(\boldsymbol{k} \times \frac{\partial \boldsymbol{V}_\mathrm{g}}{\partial z}\Big) \cdot \nabla_s \theta \\ &= -\frac{\alpha}{f}\Big(\theta_z \nabla_s \pi \cdot \nabla_s \theta + \frac{g}{\theta}|\nabla_s \theta|^2\Big), \end{aligned} \tag{7}$$

and

$$C_D = \frac{\mathrm{PV_2}}{\theta_z} = -\frac{\alpha}{f}\Big(\nabla_s \pi \cdot \nabla_s \theta + \frac{g}{\theta \theta_z}|\nabla_s \theta|^2\Big). \tag{8}$$

In the Northern Hemisphere, the geostrophic vertical vorticity f is positive, and the second term $\mathrm{PV_2^2}(= -\dfrac{\alpha}{f}\dfrac{g}{\theta}|\nabla_s \theta|^2)$ on the right hand side of Eq. (7) is negative. Although the first term $\mathrm{PV_2^1}(= -\dfrac{\alpha}{f}\theta_z \nabla_s \pi \cdot \nabla_s \theta)$ is not necessarily negative, its magnitude is usually smaller compared with the second term $\mathrm{PV_2^2}$, so $\mathrm{PV_2}$ is almost negative in the troposphere under the geostrophic balance. Figure 1 presents the three-dimensional distributions of C_D and $\mathrm{PV_2}$ under the real weather condition at 0600 UTC 22 July 2008. The distributions for other time slices are similar. It demonstrates that both C_D and $\mathrm{PV_2}$ are usually negative through out the troposphere. Therefore, using $C_D < 0$ alone as the criterion of SVD is inappropriate. For more general cases, the influence of the change in static stability needs to be considered.

In the study of Zheng et al. (2013), the equation for vertical vorticity development was deduced from a Lagrangian perspective as follows:

$$\begin{aligned} \frac{D\eta_z}{Dt} &= \frac{D}{Dt}\Big(\frac{\mathrm{PV_e} - \mathrm{PV_2}}{\theta_z}\Big) \\ &= \frac{1}{\theta_z}\frac{D\mathrm{PV_e}}{Dt} - \frac{1}{\theta_z}\frac{D\mathrm{PV_2}}{Dt} - \frac{\eta_z}{\theta_z}\frac{D\theta_z}{Dt}. \end{aligned} \tag{9}$$

It was demonstrated that the first term on the right hand side of Eq. (9), which is associated with

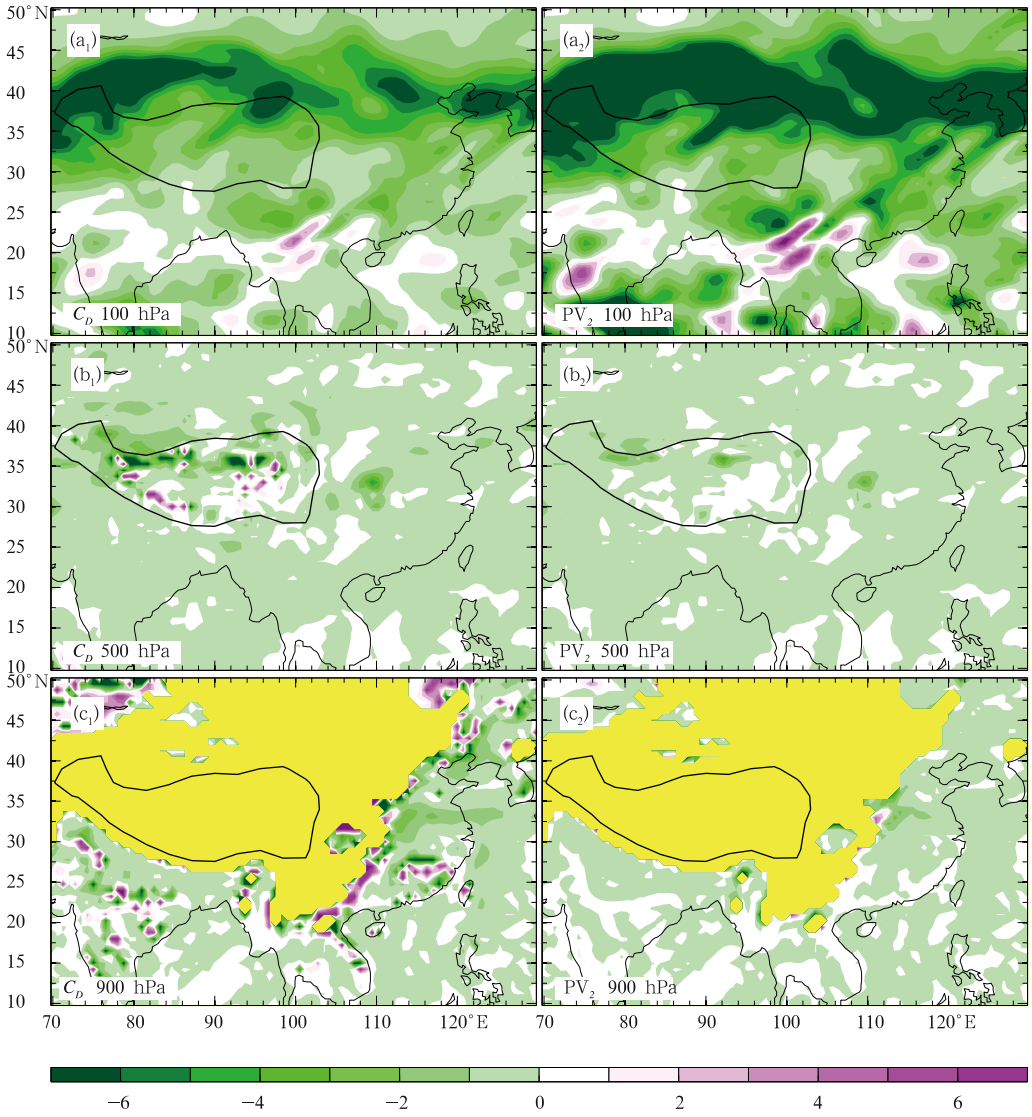

Fig. 1. Distributions at 100 hPa (a_1, a_2), 500 hPa (b_1, b_2), and 900 hPa (c_1, c_2) of C_D (a_1, b_1, c_1; 10^{-5} $m^3(kg\ s)^{-1}$) and PV_2 (a_2, b_2, c_2; 10^{-1}PVU, 1 PVU=$10^{-6}m^2$ K $(kg\ s)^{-1}$) at 0600 UTC 22 July 2008. Yellow masks the region underneath the ground surface, the same for following figures.

the diabatic heating, plays a leading role in the development and movement of a vortex. However, in some stages of the vortex development, the other terms, which are associated with the internal thermal structure of the atmosphere and can be interpreted by using SVD, can play comparable roles as the diabatic heating in the vortex development. Actually, SVD usually occurs at the initial stage of a vortex development before precipitation starts. When the vortex has developed to some extent, vertical rising develops within the vortex and precipitation appears, leading to the condensation diabatic heating, thereby enhancing the development of the vortex. In this regard, it is more important and practical to understand how SVD occurs in a more general circumstance from the Lagrangian perspective.

In Section 2, the SVD of a particle moving along a tilted isentropic surface is studied. The GSVD from a Lagrangian perspective is investigated in Section 3, and the necessary and sufficient condition for VD and SVD is clarified under the GSVD framework. In Section 4, the GSVD just developed is used to diagnose a vortex that developed over the TP then moved down to the Sichuan basin in July 2008. The relative

contributions to vertical vorticity development of the changes in both horizontal potential vorticity PV_2 and static stability θ_z are also analyzed. Conclusions and discussion are summarized in Section 5.

2. Slantwise vorticity development on a sloping isentropic surface

Define $\beta \in [0, \frac{\pi}{2})$ as the acute angle between $\nabla\theta$ and the vertical direction, i.e., $\tan\beta = \dfrac{\theta_s}{|\theta_z|}$, and define $\varrho \in [0, \pi]$ as the angle between horizontal vorticity $\boldsymbol{\eta}_s$ and baroclinity $\boldsymbol{\theta}_s$. Then

$$\begin{cases} C_D = \dfrac{\eta_s\theta_s\cos\varrho}{\theta_z} = +\eta_s\cos\varrho\tan\beta, \text{ if } \theta_z > 0, & \text{(10a)} \\ C_D = \dfrac{\eta_s\theta_s\cos\varrho}{\theta_z} = -\eta_s\cos\varrho\tan\beta, \text{ if } \theta_z < 0, & \text{(10b)} \end{cases}$$

where $\eta_s = |\boldsymbol{\eta}_s|$ and $\theta_s = |\boldsymbol{\theta}_s|$.

$$\nabla\theta = \theta_x\boldsymbol{i} + \theta_y\boldsymbol{j} + \theta_z\boldsymbol{k} = \theta_s\boldsymbol{s} + \theta_z\boldsymbol{k} = \theta_n\boldsymbol{n}, \qquad (11)$$

where $\theta_n = |\nabla\theta|$, the unit vector $\boldsymbol{n}$ is the direction of $\nabla\theta$, and the unit vector $\boldsymbol{s}$ is the direction of $\nabla_s\theta$.

Then

$$\begin{cases} \mathrm{PV_e} = \boldsymbol{\eta}_a \cdot \nabla\theta = \eta_n\theta_n > 0, \\ \qquad \Rightarrow \ \eta_n > 0, \text{ if } \theta_z > 0, & \text{(12a)} \\ \mathrm{PV_e} = \boldsymbol{\eta}_a \cdot \nabla\theta = \eta_n\theta_n < 0, \\ \qquad \Rightarrow \ \eta_n < 0, \text{ if } \theta_z < 0, & \text{(12b)} \end{cases}$$

where $\eta_n = \boldsymbol{\eta}_a \cdot \boldsymbol{n}$ is the projection of absolute vorticity $\boldsymbol{\eta}_a$ on the direction of $\boldsymbol{n}$.

Therefore, Eq. (1) can be written as

$$\begin{cases} \eta_z = +\dfrac{\eta_n}{\cos\beta} - \eta_s\cos\varrho\tan\beta, \text{ if } \theta_z > 0, & \text{(13a)} \\ \eta_z = -\dfrac{\eta_n}{\cos\beta} + \eta_s\cos\varrho\tan\beta, \text{ if } \theta_z < 0. & \text{(13b)} \end{cases}$$

If $C_D < 0$, Eq. (10) yields

$$\begin{cases} \cos\varrho < 0, \quad \Rightarrow \quad \varrho \in \left(\dfrac{\pi}{2}, \pi\right], \quad \text{if } \theta_z > 0, & \text{(14a)} \\ \cos\varrho > 0, \quad \Rightarrow \quad \varrho \in \left[0, \dfrac{\pi}{2}\right), \quad \text{if } \theta_z < 0, & \text{(14b)} \end{cases}$$

since both η_s and $\tan\beta$ are positive.

Using Eqs. (14) and (12), Eq. (13) can be written as

$$\eta_z = \frac{|\eta_n|}{\cos\beta} + \eta_s|\cos\varrho|\tan\beta. \qquad (15)$$

Under the constraint of $C_D < 0$, taking derivative of Eq. (15) with respect to β leads to

$$\frac{D\eta_z}{D\beta} = \left(\frac{|\eta_n|\sin\beta}{\cos^2\beta} + \frac{\eta_s|\cos\varrho|}{\cos^2\beta}\right) + \left(\frac{D|\eta_n|}{D\beta}\frac{1}{\cos\beta} + \frac{D\eta_s}{D\beta}|\cos\varrho|\tan\beta + \eta_s\frac{D|\cos\varrho|}{D\beta}\tan\beta\right). \qquad (16)$$

The terms in the first parenthesis on the right hand side of Eq. (16) are second order positive infinite but the terms in the second parenthesis are first order positive or negative infinite when β approaches $\frac{\pi}{2}$, thus

$$\frac{D\eta_z}{D\beta} \to \infty, \quad \text{if } \beta \to \frac{\pi}{2}, \qquad (17)$$

which demonstrates that when an air particle is sliding down the concave slope or up the convex slope of an isentropic surface and $C_D < 0$, its vertical vorticity will increase rapidly.

Assuming the directions of horizontal vorticity $\boldsymbol{\eta}_s$ and baroclinity $\boldsymbol{\theta}_s$ are strictly opposite (identical) for a stable (unstable) atmosphere, i.e., $\varrho = \pi$ ($\varrho = 0$) for $\theta_z > 0$ ($\theta_z < 0$), then $C_D < 0$; and assuming θ_n is constant, then η_n is constant, since $\mathrm{PV_e} = \eta_n\theta_n$ is conserved. Thus, Eq. (15) becomes

$$\eta_z = \frac{|\eta_n|}{\cos\beta} + \eta_s\tan\beta \Rightarrow \eta_z \to \infty, \text{ if } \beta \to \frac{\pi}{2}, \qquad (18)$$

which is illustrated schematically in Fig. 2 (Fig. 3) for the downsliding SVD in the stable (unstable) atmosphere. Equation (18) can be used to explain the upsliding SVD in the stable or unstable atmosphere. Since there is no essential difference between downsliding SVD and upsliding SVD, the schematic diagram for upsliding SVD is not shown here. An air particle at the initial position A^0 possesses zero C_D since the isentropic surface is horizontally located. During the adiabatic movement of the particle, because the directions of horizontal vorticity $\boldsymbol{\eta}_s$ and baroclinity $\boldsymbol{\theta}_s$ are strictly opposite (identical) for a stable (unstable) atmosphere, when the particle moves from A^0 to A at the same isentropic surface, its vertical absolute vorticity η_z is increased.

It is worthy a note that the above analysis is just a qualitative demonstration of the SVD conception. Under the premise $C_D < 0$, vertical vorticity will increase dramatically when a particle is moving along a sharply tilted isentropic surface (i.e., β increases rapidly).

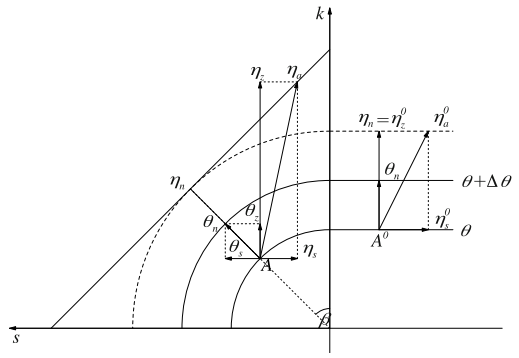

Fig. 2. Schematic diagram showing the development of vertical vorticity in a stable atmosphere owing to the slantwise sloping of the isentropic surface when the directions of horizontal vortical $\boldsymbol{\eta}_s$ and baroclinity $\boldsymbol{\theta}_s$ are opposite. Initially, a particle is at position A^0 on the horizontal part of a θ surface, and $\mathrm{PV_e}(=\eta_n\theta_n)$ is conserved. When it slides down the θ surface at an angle β to position A, due to $\eta_z=\dfrac{|\eta_n|}{\cos\beta}+\eta_s\tan\beta$, the increasing in β can result in the development of η_z.

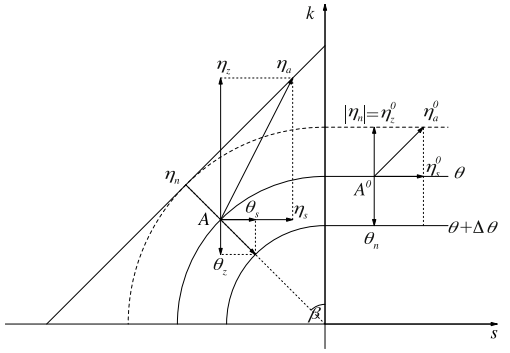

Fig. 3. As in Fig. 2, but for the unstable atmosphere case when the directions of horizontal vortical $\boldsymbol{\eta}_s$ and baroclinity $\boldsymbol{\theta}_s$ are strictly identical.

3. Generalized slantwise vorticity development (GSVD)

The above SVD theory is based on isentropic coordinate with a priori assumption that the sloping angle β of isentropic surface increases with time. Since $\dfrac{D\eta_z}{Dt}=\dfrac{D\eta_z}{D\beta}\dfrac{D\beta}{Dt}$, the change of the tilting angle β of the isentropic surface has to be analyzed as well. This is inconvenient and usually ignored in the application of SVD. For practical reasons and making it move general, the SVD will be studied from a Lagrangian perspective.

3.1 Vorticity development (VD)

Taking derivative of Eq. (1) with respect to time under the constraint of the conservation of Ertel potential vorticity leads to

$$\left(\frac{D\eta_z}{Dt}\right)_A=-\frac{\mathrm{PV_e}}{\theta_z^2}\frac{D\theta_z}{Dt}-\frac{DC_D}{Dt},\quad \theta_z\neq 0, \tag{19}$$

where $\left(\dfrac{D\eta_z}{Dt}\right)_A$ denotes the adiabatic development of vertical vorticity. Thus, the necessary and sufficient condition for VD is

$$\frac{DC_D}{Dt}<-\frac{\mathrm{PV_e}}{\theta_z^2}\frac{D\theta_z}{Dt},\quad \theta_z\neq 0. \tag{20}$$

This is the condition given in Eq. (3) by Wu and Liu (1997) but in a different form.

3.2 Slantwise vorticity development (SVD)

$$\text{If}\qquad \frac{DC_D}{Dt}<0, \tag{21}$$

Eq. (19) can be written as

$$\left(\frac{D\eta_z}{Dt}\right)_A=-\frac{\mathrm{PV_e}}{\theta_z^2}\frac{D\theta_z}{Dt}+\left|\frac{DC_D}{Dt}\right|,\quad \theta_z\neq 0. \tag{22}$$

$$\text{If}\qquad \frac{DC_D}{Dt}<0<-\frac{\mathrm{PV_e}}{\theta_z^2}\frac{D\theta_z}{Dt},\quad \theta_z\neq 0, \tag{23}$$

Eq. (22) yields

$$\left(\frac{D\eta_z}{Dt}\right)_A\to\infty,\quad \text{if } |\theta_z|\to 0. \tag{24}$$

This implies that when Eq. (23) is satisfied, the vertical vorticity of an air particle can develop rapidly if the atmospheric static stability approaches neutral.

In general, in an inertial stable atmosphere, the signs of $\mathrm{PV_e}$ and θ_z are identical. In such circumstances, Eq. (23) can be interpreted as:

$$\begin{cases}\dfrac{D\theta_z}{Dt}<0 \text{ and } \dfrac{DC_D}{Dt}<0, \text{ if } \theta_z>0, & \text{(25a)}\\[2ex] \dfrac{D\theta_z}{Dt}>0 \text{ and } \dfrac{DC_D}{Dt}<0, \text{ if } \theta_z<0, & \text{(25b)}\end{cases}$$

Therefore, the SVD can be stated as: When an air particle is sliding down the concave slope or up the convex slope of an isentropic surface in a stable stratified atmosphere with its static stability decreasing, or in an unstable atmosphere with its static stability increasing, its vertical vorticity can develop rapidly if its C_D is decreasing. That is, the vertical vorticity of

an air particle will intensify rapidly when its stability approaches zero, i.e., the particle is inclined to neutral stability, if its C_D decreases.

3.3 Relation between VD and SVD

Integration with respect to time of the necessary and sufficient condition Eq. (20) leads to

$$\Delta C_D < \int_t^{t+\Delta t} -\frac{\mathrm{PV_e}}{\theta_z^2}\frac{D\theta_z}{Dt}Dt = -\Big(\frac{\mathrm{PV_e}}{\theta_z^2}\Big)^*\Delta\theta_z, \quad \theta_z \neq 0, \tag{26}$$

where $\Delta C_D = C_D(t+\Delta t) - C_D(t)$ and $\Delta\theta_z = \theta_z(t+\Delta t) - \theta_z(t)$. Let

$$\Gamma = -\Big(\frac{\mathrm{PV_e}}{\theta_z^2}\Big)^*\Delta\theta_z, \quad \theta_z \neq 0. \tag{27}$$

For a stable atmosphere ($\theta_z > 0$, then $\mathrm{PV_e} > 0$) and a decreasing stability ($\Delta\theta_z < 0$), or for an unstable atmosphere ($\theta_z < 0$, then $\mathrm{PV_e} < 0$) and an increasing stability ($\Delta\theta_z > 0$), $\Gamma > 0$. In such a circumstance, the necessary and sufficient condition Eq. (26) for VD becomes

$$\Delta C_D < \Gamma. \tag{28}$$

On the other hand, integration with respect to time of Eq. (21) for SVD yields

$$\Delta C_D < 0. \tag{29}$$

Comparison of Eqs. (28) and (29) indicates that the demand for SVD is much more restricted than the demand for VD, and the occurrence of severe weather is much less frequent comparing with that of ordinary weather.

3.4 Relation between PV_2 and SVD

The necessary and sufficient condition Eq. (23) for SVD can be written as

$$\frac{1}{\theta_z}\frac{D\mathrm{PV_2}}{Dt} - \frac{\mathrm{PV_2}}{\theta_z^2}\frac{D\theta_z}{Dt} < 0 < -\frac{\mathrm{PV_e}}{\theta_z^2}\frac{D\theta_z}{Dt}, \quad \theta_z \neq 0. \tag{30}$$

Adding a negative term $\frac{\mathrm{PV_e}}{\theta_z^2}\frac{D\theta_z}{Dt}$ to inequality Eq. (30) and multiplying –1 lead to

$$-\frac{1}{\theta_z}\frac{D\mathrm{PV_2}}{Dt} - \frac{\eta_z}{\theta_z}\frac{D\theta_z}{Dt} > -\frac{\mathrm{PV_e}}{\theta_z^2}\frac{D\theta_z}{Dt} > 0, \quad \theta_z \neq 0. \tag{31}$$

For $\mathrm{PV_e}$ conservation, Eq. (9) becomes

$$\Big(\frac{D\eta_z}{Dt}\Big)_A = -\frac{1}{\theta_z}\frac{D\mathrm{PV_2}}{Dt} - \frac{\eta_z}{\theta_z}\frac{D\theta_z}{Dt} > -\frac{\mathrm{PV}_e}{\theta_z^2}\frac{D\theta_z}{Dt} > 0, \quad \theta_z \neq 0. \tag{32}$$

This provides the relation between SVD and the change in $\mathrm{PV_2}$, and indicates that in a stable (unstable) atmosphere, a decrease (increase) of $\mathrm{PV_2}$ will result in vertical vorticity development. The intensity of SVD depends on the change of atmospheric static stability:

$$\Big(\frac{D\eta_z}{Dt}\Big)_A > \mathrm{PV_e}\frac{D}{Dt}\Big(\frac{1}{\theta_z}\Big) > 0, \quad \theta_z \neq 0. \tag{33}$$

Equation (33) indicates that only when $\mathrm{PV_e}\frac{D}{Dt}\Big(\frac{1}{\theta_z}\Big) > 0$ and the adiabatic development $\Big(\frac{D\eta_z}{Dt}\Big)_A$ of vertical vorticity exceeds $\mathrm{PV_e}\frac{D}{Dt}\Big(\frac{1}{\theta_z}\Big)$, can VD be named as SVD. For a symmetric stable atmosphere with $\mathrm{PV_e} > 0$, when the static stability decreases to approach neutral stratification, SVD will occur, leading to the occurrence of severe weather.

4. PV-θ analysis of a Tibetan Plateau vortex

The data and computational methods used here are the same as those used in Part I of this study (Zheng et al., 2013). In Part I, Eq. (9) was employed to diagnose the development and movement of a TPV, which was generated over the TP before 20 July 2008, and slid down the TP after 1800 UTC 21 July 2008, then propagated eastward along the Yangtze River, resulting in heavy precipitation along with the vortex. The results (Figs. 5 and 6 in Part I) demonstrated that the contribution of $\frac{1}{\theta_z}\frac{D\mathrm{PV_e}}{Dt}$ due to the change in PV_e is analogous to the total change $\frac{D\eta_z}{Dt}$ of vertical vorticity with the same order of magnitudes; the positive center of the contribution of $-\frac{1}{\theta_z}\frac{D\mathrm{PV_2}}{Dt}$ due to the change in $\mathrm{PV_2}$ is coincident with the development center of vertical vorticity of the TPV, though weaker in magnitude; whereas the contribution of $-\frac{\eta_z}{\theta_z}\frac{D\theta_z}{Dt}$ due to the change of static stability θ_z to the development of vertical vorticity is negative and is weaker in magnitude for the static stability θ_z increasing in a

stable atmosphere, or is positive and weaker in magnitude for the static stability θ_z decreasing (increasing) in a stable (unstable) atmosphere.

It was also demonstrated that it is the heterogeneity in both vertical and horizontal directions of the diabatic heating that plays a leading role in the development and movement of the TPV. However, in some stage of the vortex's evolution, the adiabatic term $-\frac{1}{\theta_z}\frac{D\mathrm{PV}_2}{Dt}$ played a significant role in the vortex's development, which is comparable with the role

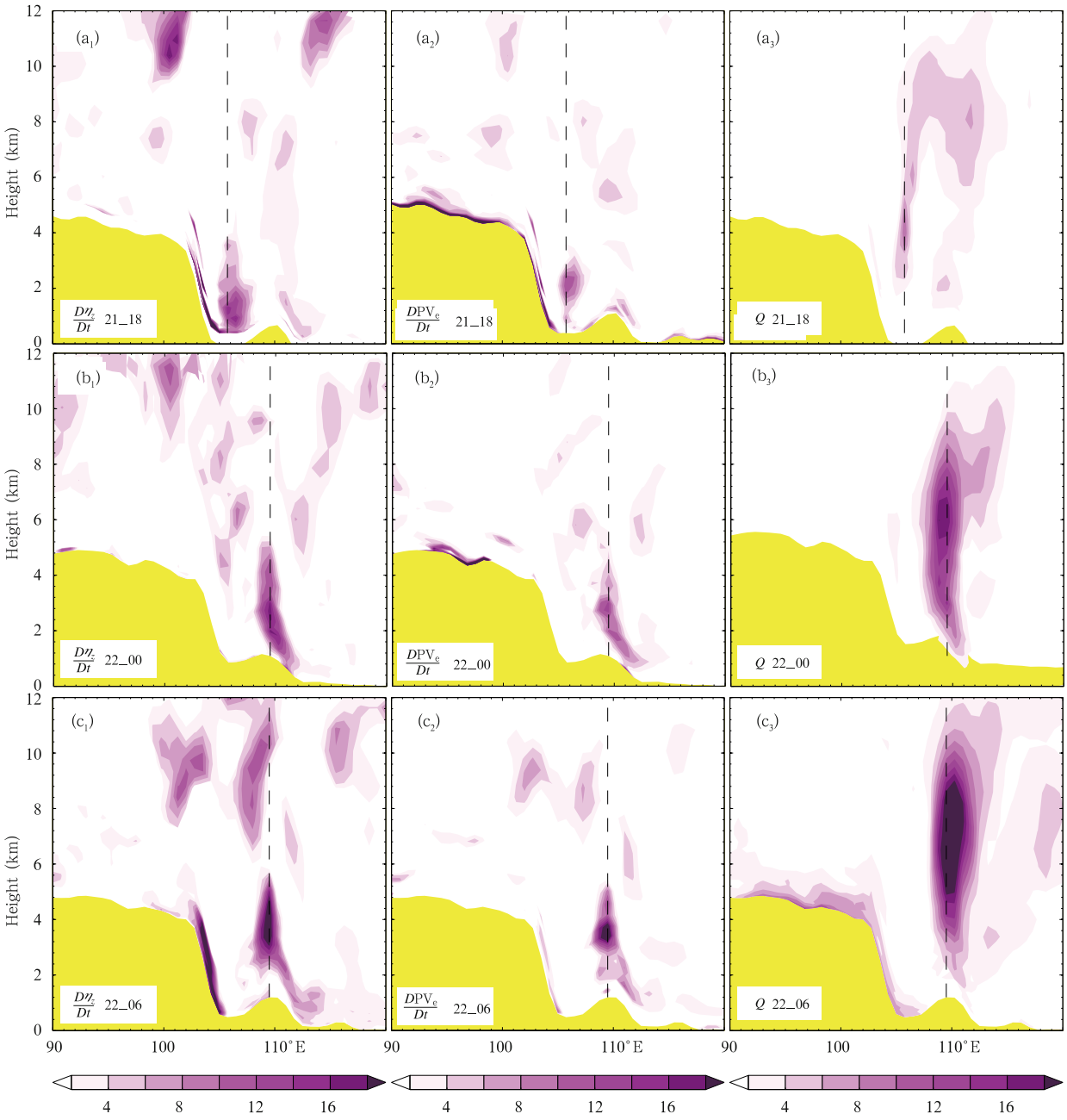

Fig. 4. Zonal vertical cross-sections across the center of the TPV at (a_1, a_2, a_3) 1800 UTC 21, (b_1, b_2, b_3) 0000 UTC 22, and (c_1, c_2, c_3) 0600 UTC 22 July 2008. The vertical dashed line denotes the center of TPV. The shadings in left, middle, and right columns are the Lagrangian change of η_z ($\frac{D\eta_z}{Dt}$; 10^{-5} m^3 (kg s 6 h)$^{-1}$), the Lagrangian change of $\mathrm{PV_e}$($\frac{D\mathrm{PV_e}}{Dt}$; 10^{-1} PVU (6 h)$^{-1}$), and Q (K (6 h)$^{-1}$), respectively.

of diabatic heating. One example is selected on 22 July 2008 when the vortex was climbing the upslope of the mountain range over the northeastern Sichuan Province. As shown in Fig. 2 in Part I (Zheng et al., 2013), the area average precipitation associated with the TPV reached a maximum of 13 mm in 6 h at 0000 UTC 22 July 2008, and the vertical relative vorticity of the TPV was intensified to a maximum 2×10^{-4} s^{-1} at 0600 UTC 22 July 2008. Figure 4 shows the distributions of the total change in vertical vorticity η_z, the change in potential vorticity $\mathrm{PV_e}$, and the diabatic heating Q for this period, which are adopted from Fig. 7 in Part I. The evolutions of vertical vorticity development (left panels) and diabatic heating Q (right panels) of the TPV indicate that its intensity and precipitation developed rapidly in this 12-h interval. More importantly, the contribution to this development from the diabatic

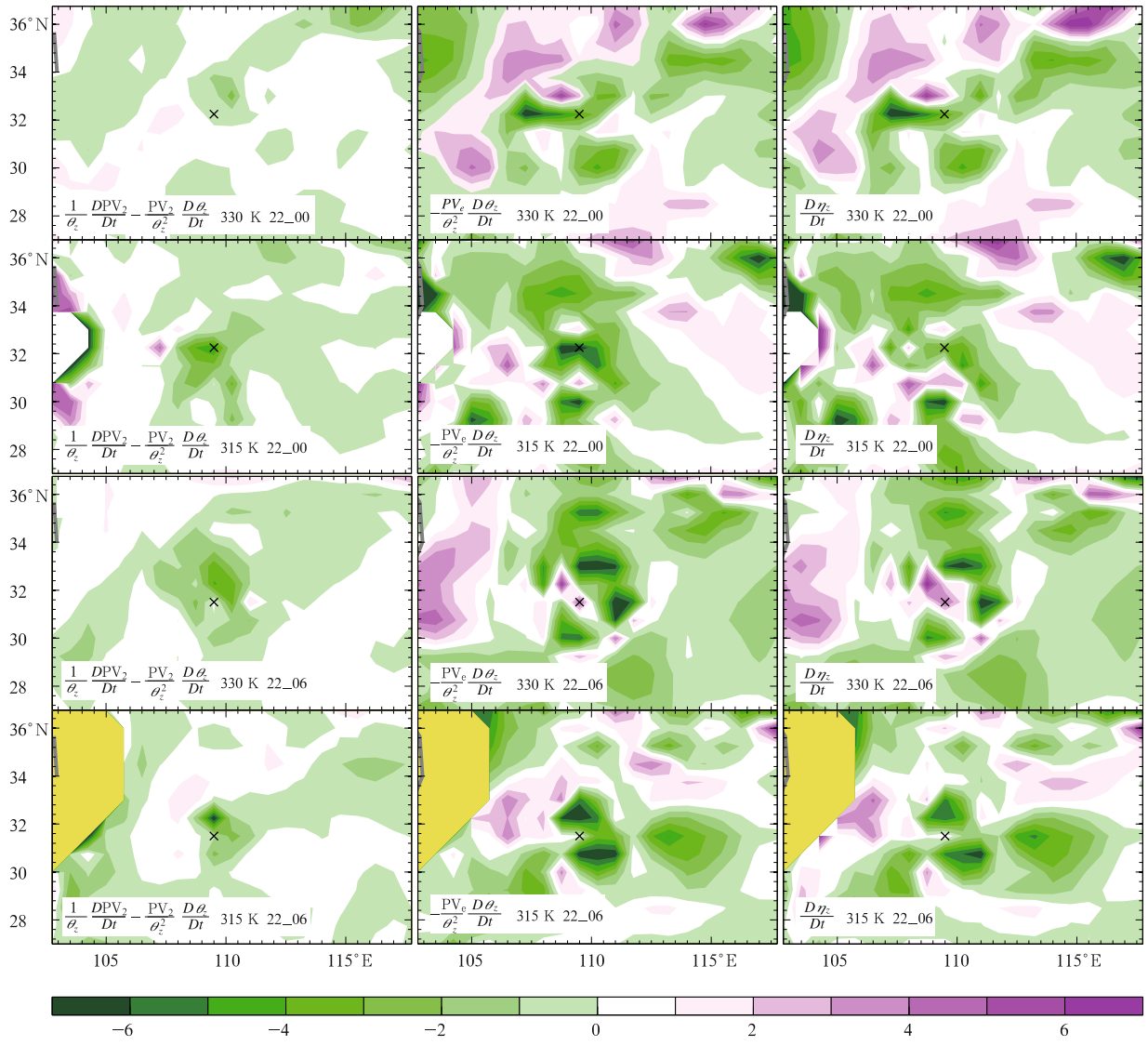

Fig. 5. Distributions on the 330- and 315-K isentropic surfaces of $\dfrac{DC_D}{Dt} = \dfrac{1}{\theta_z}\dfrac{D\mathrm{PV_2}}{Dt} - \dfrac{\mathrm{PV_2}}{\theta_z^2}\dfrac{D\theta_z}{Dt}$ (left column), $\gamma = -\dfrac{\mathrm{PV_e}}{\theta_z^2}\dfrac{D\theta_z}{Dt}$ (middle column), and $\left(\dfrac{D\eta_z}{Dt}\right)_A = \gamma - \dfrac{DC_D}{Dt}$ (right column) at (a) 0000 UTC and (b) 0600 UTC 22 July 2008. The unit of shading is 10^{-5} m^3(kg s 6 h)$^{-1}$. The cross means the location of the TPV, the same for following figures.

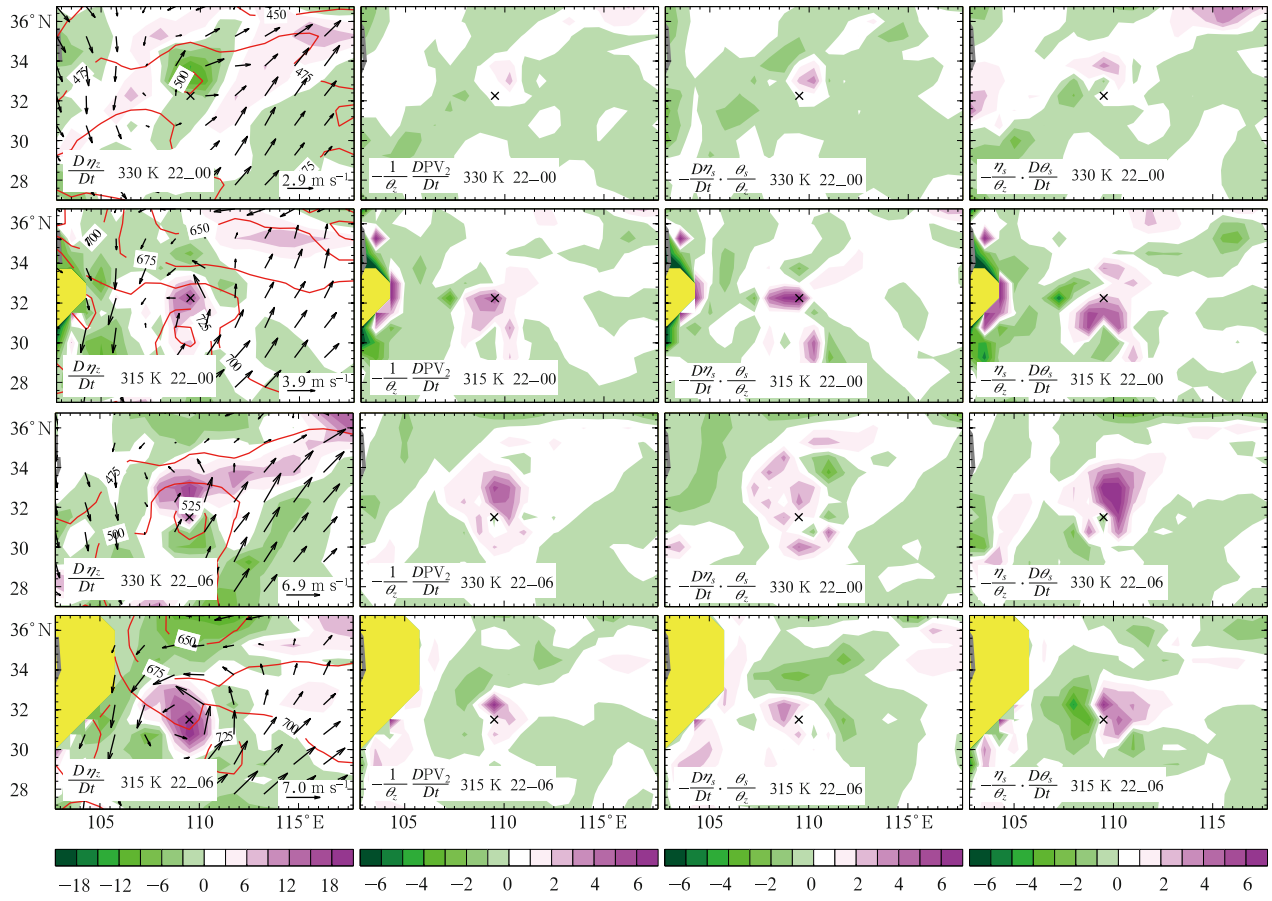

Fig. 6. Development of vertical vorticity η_z (left column; 10^{-5} m^3(kg s 6 h)$^{-1}$), and the associated contributions due to the changes in horizontal potential vorticity ($-\frac{1}{\theta_z}\frac{D\mathrm{PV}_2}{Dt}$; middle left column), horizontal vorticity ($-\frac{\boldsymbol{\theta}_s}{\theta_z}\cdot\frac{D\boldsymbol{\eta}_s}{Dt}$; middle right column), and baroclinity ($-\frac{\boldsymbol{\eta}_s}{\theta_z}\cdot\frac{D\boldsymbol{\theta}_s}{Dt}$; right column) at (a) 0000 UTC and (b) 0600 UTC 22 July 2008. The contour and vector in the first column are pressure in hPa and horizontal wind, respectively. The unit of shading in the last three columns is 0.5×10^{-5}m^3(kg s 6 h)$^{-1}$.

term $\frac{1}{\theta_z}\frac{D\mathrm{PV_e}}{Dt}$ (middle panels) is significant: its intensity at each time step is close to the total change $\frac{D\eta_z}{Dt}$ in vertical vorticity η_z. Besides, the height of its maximum center also increases from 2 km at 1800 UTC 21 July 2008 to 3 km at 0000 UTC 22 July 2008, and reaches 4 km 6 h later, contributing to the vertical extension of the vortex.

Figure 5 shows the distributions on the 330- and 315-K isentropic surfaces of the terms $\frac{DC_D}{Dt} = \frac{1}{\theta_z}\frac{D\mathrm{PV}_2}{Dt} - \frac{\mathrm{PV}_2}{\theta_z^2}\frac{D\theta_z}{Dt}$, $\gamma = -\frac{\mathrm{PV_e}}{\theta_z^2}\frac{D\theta_z}{Dt}$, and $\left(\frac{D\eta_z}{Dt}\right)_A = \gamma - \frac{DC_D}{Dt}$ at 0000 and 0600 UTC 22 July 2008. It shows that at 0000 UTC on both the 330- and 315-K surfaces, in the region surrounding the vortex center, $\frac{DC_D}{Dt} > \gamma$ and $\left(\frac{D\eta_z}{Dt}\right)_A < 0$, implying the criteria Eq. (20) for VD is unsatisfied, and the vortex development at 0000 UTC is basically due to the diabatic heating as diagnosed in Part I. At 0600 UTC on the 315-K surface at the vortex center, $\frac{DC_D}{Dt} < \gamma$ and $\left(\frac{D\eta_z}{Dt}\right)_A > 0$, implying the criteria Eq. (20) for VD is satisfied, and the development of vortex in the lower layer is at least partly due to contribution under an adiabatic environment. On the other hand, since $\gamma < 0$ at this level, the SVD criteria Eq. (23) is violated, so the vortex adiabatic development is limited. On the 330-K surface at the vortex center, not only

$\frac{DC_D}{Dt} < \gamma$, but also $\frac{DC_D}{Dt} < 0 < \gamma$. These indicate that the criteria Eq. (20) and Eq. (23) are satisfied, thus both VD and SVD occur. This is consistent with the upward intensification of the TPV at 0600 UTC 22 July 2008 (Fig. 4).

As shown in Eq. (32), the vertical vorticity development $\left(\frac{D\eta_z}{Dt}\right)_A$ under adiabatic condition is composed of two parts: the part $\left(-\frac{1}{\theta_z}\frac{D\mathrm{PV}_2}{Dt}\right)$ due to the change in horizontal component PV_2 of potential vorticity and the part $\left(-\frac{\eta_z}{\theta_z}\frac{D\theta_z}{Dt}\right)$ due to the change in static stability θ_z. The part of adiabatic development of vertical vorticity due to the change in PV_2 can be expressed as

$$\left(\frac{D\eta_z}{Dt}\right)_{\mathrm{PV}_2} = -\frac{1}{\theta_z}\frac{D\mathrm{PV}_2}{Dt} = -\frac{1}{\theta_z}\frac{D(\boldsymbol{\eta}_s\cdot\boldsymbol{\theta}_s)}{Dt} = -\frac{D\boldsymbol{\eta}_s}{Dt}\cdot\frac{\boldsymbol{\theta}_s}{\theta_z} - \frac{\boldsymbol{\eta}_s}{\theta_z}\cdot\frac{D\boldsymbol{\theta}_s}{Dt}, \quad \theta_z \neq 0. \quad (34)$$

Figure 6 demonstrates the spatial distributions of these three terms in Eq. (34), besides the total change of vertical vorticity at the 330- and 315-K isentropic surfaces on 22 July 2008. It is evident that both the contributions to the development of vertical vorticity due to the change in horizontal vorticity $\boldsymbol{\eta}_s$ and that due to the change in baroclinity $\boldsymbol{\theta}_s$ are positive. As shown in Fig. 1, $\mathrm{PV}_2 = \boldsymbol{\eta}_s\cdot\boldsymbol{\theta}_s$ is commonly negative, that is, the directions of $\boldsymbol{\eta}_s$ and $\boldsymbol{\theta}_s$ are opposite. The positive contributions of the two terms on the right hand side of Eq. (34) imply that the change of $\boldsymbol{\eta}_s$ is opposite to the direction of $\boldsymbol{\theta}_s$, and the change of $\boldsymbol{\theta}_s$ is opposite to the direction of $\boldsymbol{\eta}_s$ during the development of vertical vorticity. Thus, either the component of horizontal vorticity $\boldsymbol{\eta}_s$ or that of baroclinity $\boldsymbol{\theta}_s$ along the project direction is increasing when vertical vorticity develops. This confirms the conclusion of Wu and Liu (1997) that the development of vertical vorticity is not necessary associated with the vorticity conversion from its horizontal to vertical component owing to the uneven lifting of a vortex. In other words, an increase in vertical vorticity may not require a decrease in horizontal vorticity, and can be achieved as well by the increasing of either horizontal vorticity or baroclinity along project direction. In summary, both the dynamical effect of horizontal vorticity $\boldsymbol{\eta}_s$ and the thermal effect of $\boldsymbol{\theta}_s$ have positive contributions to the development of vertical vorticity.

5. Conclusions and discussion

While Part I of this study (Zheng et al., 2013) focused on the vertical vorticity development due to atmospheric diabatic heating, the current study concentrates on the development of vertical vorticity under adiabatic condition from the view of potential vorticity and potential temperature (PV–θ) and from a Lagrangian perspective.

First, it is highlighted that since in most cases, the troposphere atmosphere is statically stable and under geostrophic balance, C_D and PV_2 are usually negative. Thus, merely using $C_D < 0$ as a condition for SVD on isentropic surface is incomplete, whereas an increase in the titling angle β of isentropic surface is required. The latter concerns the changes in both baroclinity $\boldsymbol{\theta}_s$ and static stability θ_z, and is inconvenient in operational or practical use.

A new concept of generalized slantwise vorticity development (GSVD) is introduced from a Lagrangian perspective, which can be used in any coordinate system. The criteria for VD and SVD are also developed, respectively, to distinguish between VD and SVD. VD requires $\frac{DC_D}{Dt} < \gamma$, in which $\gamma = -\frac{\mathrm{PV_e}}{\theta_z^2}\frac{D\theta_z}{Dt}$, $\theta_z \neq 0$; whereas SVD requires $\frac{DC_D}{Dt} < 0 < \gamma$. It demonstrates that the demand for SVD is much more restricted than that for VD; correspondingly, $\frac{D\eta_z}{Dt} > 0$ under VD whereas $\frac{D\eta_z}{Dt} > \mathrm{PV_e}\frac{D}{Dt}\left(\frac{1}{\theta_z}\right)$ under SVD. This accounts for the frequent occurrences of frontal and cyclonic systems and the sparsity of severe weather. Under the GSVD framework, when an air particle is sliding down the concave slope or up the convex slope of an isentropic surface in a stable stratified atmosphere with its static stability decreasing, or in an unstable atmosphere with its static stability increasing, its vertical vorticity can develop rapidly if its C_D is decreasing. That is, the vertical vorticity of an air particle will intensify rapidly when its stability approaches zero, i.e., the particle is inclined to neutral stability, if its C_D decreases. The intensity of vertical vorticity development due to SVD is estimated as $\frac{D\eta_z}{Dt} > \mathrm{PV_e}\frac{D}{Dt}\left(\frac{1}{\theta_z}\right)$, which indicates that when the atmosphere approaches neutral stratification, the development of vertical vorticity

approaches infinity.

These theoretical results are used to analyze the development of a TPV which appeared over the TP, then slid down and moved eastward in late July 2008, resulting in heavy rainfall in Sichuan Province. At some stages of the vortex development, the VD criteria are violated, implying that the vortex development depends solely on the diabatic heating as discussed in Part I (Zheng et al., 2013). At some stages, the VD criteria are satisfied while the SVD criteria are violated, and the adiabatic development of the vortex is limited. At one moment, i.e., 0600 UTC 22 July 2008, on the 330-K isentropic surface, both VD and SVD criteria are satisfied, and the adiabatic development of vertical vorticity contributes to the upward development of the vortex. It is further demonstrated that the change of PV_2 contributes to the intensification of the TPV from 0000 to 0600 UTC 22 July 2008 when it slid upward on the upslope of the northeastern edge of the Sichuan basin since the changes in both horizontal vorticity $\boldsymbol{\eta}_s$ and baroclinity $\boldsymbol{\theta}_s$ have positive effects on the development of vertical vorticity.

The appearance of the stronger signals concerning VD and SVD in the region surrounding the vortex compared to other parts of the troposphere indicates that the GSVD concept can serve as a useful tool for diagnosing the development of severe weather systems. As the SVD concept has been extended to a saturated moist atmosphere (Wu et al., 1995) and can be extended to an unsaturated moist atmosphere (Gao et al., 2004), the concept of GSVD in a moist atmosphere should be extended in future to investigate the mechanism of the formation and development of severe weather such as the gullywasher in summer.

This paper discusses the adiabatic development of vertical vorticity where the static stability θ_z plays a significant role under the constraint of conservation of potential vorticity when the weather system moves along the slope of the isentropic surface. While the first part (Zheng et al., 2013) investigates the effect of diabatic heating on the development of vertical vorticity and points out by case study that diabatic heating plays a leading role on the development of vertical vorticity in most occasions, in real atmosphere, diabatic heating and static stability can interact in a complex manner where there is complicated feedback. It is significant and challenging to further investigate the effect of this feedback on the development of weather system.

REFERENCES

Chen Zhongming, Min Wenbin, Xu Maoliang, et al., 2004: Mesoscale characteristics of the unbalanced force of atmospheric motion and environmental fields of rain storm on 20–21 July 1998. *Acta Meteor. Sinica*, **62**, 375–383. (in Chinese)

Cui Xiaopeng, Wu Guoxiong, and Gao Shouting, 2002: Numerical simulation and isentropic analysis of frontal cyclones over the western Atlantic Ocean. *Acta Meteor. Sinica*, **60**, 385–399. (in Chinese)

——, Gao Shouting, and Wu Guoxiong, 2003: Up-sliding slantwise vorticity development and the complete vorticity equation with mass forcing. *Adv. Atmos. Sci.*, **20**, 825–836.

Gao, S., X. Wang, and Y. Zhou, 2004: Generation of generalized moist potential vorticity in a frictionless and moist adiabatic flow. *Geophys. Res. Lett.*, **31**, L12113.

Hoskins, B., M. Mclntyre, and A. Robertson, 1985: On the use and significance of isentropic potential vorticity maps. *Quart. J. Roy. Meteor. Soc.*, **111**, 877–946.

Jiang Yongqiang, Chen Zhongyi, Zhou Zuguang, et al., 2004: Slantwise vorticity development and meso-β scale low vortex. *Journal of PLA University of Science and Technology*, **5**, 81–87.

Ma Leiming, Qin Zengying, Duan Yihong, et al., 2002: Case study on the impact of atmospheric baroclinicity to the initial development of Jianghuai cyclones. *Acta Oceanologica Sinica*, **24**, 95–104.

Wang Ying, Wang Yan, Zhang Lixiang, et al., 2007: The development of slantwise vorticity near a weakened tropical cyclone. *J. Trop. Meteor.*, **23**, 47–52. (in Chinese)

Wu Guoxiong, Cai Yaping, and Tang Xiaojing, 1995: Moist potential vorticity and slantwise vorticity development. *Acta Meteor. Sinica*, **53**, 387–405. (in Chinese)

——, and H. Liu, 1997: Vertical vorticity development owing to down-sliding at slantwise isentropic surface. *Dyn. Atmos. Oceans.*, **27**, 715–743.

Zheng Yongjun, Wu Guoxiong, and Liu Yimin, 2013: Dynamical and thermal problems in vortex development and movement. Part I: A PV–Q view. *Acta Meteor. Sinica*, **27**(1), 1–14.